THE RHT CONCRETE MODEL IN LS-DYNA

Dr. Thomas Borrvall
Engineering Research Nordic AB
Linköping, Sweden
thomas.borrvall@erab.se

Dr. Werner Riedel
Fraunhofer Institut fur Kurzzeitdynamik, Ernst-Mach-Institut
Freiburg, Germany

Abstract

The RHT concrete model is implemented in LS-DYNA. It is a macro-scale material model that incorporates features that are necessary for a correct dynamic strength description of concrete at impact relevant strain rates and pressures. The shear strength of the model is described by means of three limit surfaces; the inelastic yield surface, the failure surface and the residual surface, all dependent on the pressure. The post-yield and post-failure behaviors are characterized by strain hardening and damage, respectively, and strain rate effects is an important ingredient in this context. Furthermore, the pressure is governed by the Mie-Gruneisen equation of state together with a p-α model to describe the pore compaction hardening effects and thus give a realistic response in the high pressure regime. Validations have been performed on smaller test examples and a contact detonation application is presented to illustrate the performance of the proposed model.

1. Introduction

Dynamic strength analysis and modelling of concrete is a challenging field that has drawn a fair amount of attention the last few decades. Experiments for relevant loading rates and pressures reveal that concrete exhibits a complicated nonlinear behavior that is difficult to capture in a single constitutive model. Much of the nonlinearity stems from the mesomechanical composition of concrete and the internal processes resulting therefrom, such as porous compaction, complex strain localization, microcracking, cell wall buckling and plasticity, just to name a few. These micromechanical effects need a homogenized macromechanical description that will involve the appropriate interdependence between stress, strain, plastic strain, strain rate, damage and failure in order to be implemented and used in a general purpose finite element code such as LS-DYNA [1]. A number of models have been proposed to describe concrete in this context, out of which, e.g., Holmqvist and Johnson [2] and Malvar et.al. [4] have been available for some time in LS-DYNA. As a complement to the already existing models, we here couple an equation-of-state that accounts for the porous compaction of concrete [5,6] with the RHT strength model [3]. The paper is organized as follows. In Section 2 and 3 we give a qualitative overview of the model before presenting the mathematical details in Section 5. The mathematical description is preceeded with the keyword format together with an example of parameter settings for a standard concrete in Section 4 and a numerical example is presented in Section 6. The paper ends with a summary and outlook in Section 7.

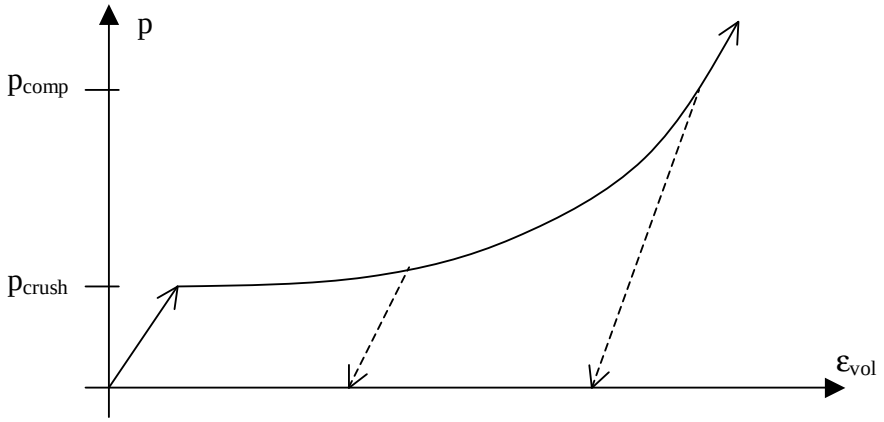

Figure 1 Schematical description of the p-α equation of state

2. The p-α compaction model

The schematical description of the volumetric compaction model is shown in Figure 1, where the pore crush pressure and compaction pressure play important roles. The porous compaction starts at a pressure value corresponding to the pore crush pressure, below which the model is elastic. On the initiation of pore collapse, a significant reduction in the effective bulk modulus is observed as the related micromechanical effects reduce the volumetric stiffness of the material. An internal variable α represents the porosity of the material as the fraction between the density of the matrix material and the porous concrete, and will thus decrease with increasing pressure and make the loading process irreversible. Unloading beyond the pore crush pressure occurs along the current elastic stiffness and will result in a permanent volumetric strain for zero pressure, subsequent reloading occurs along the unloading curve. When the pressure reaches the compaction pressure the material is assumed fully compacted (α=1) and will be governed by a conventional equation of state model.

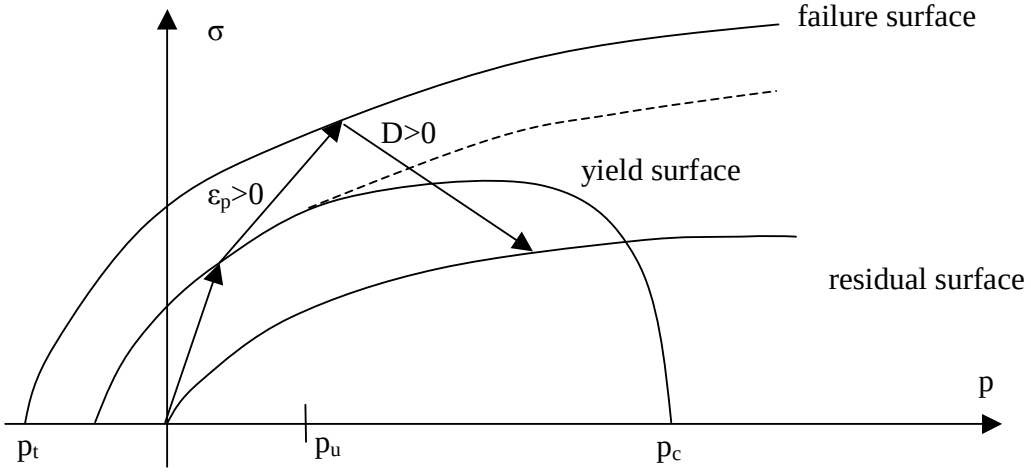

Figure 2 Stress limit surfaces and loading scenario in the RHT strength model

3. The RHT strength model

The RHT strength model is expressed in terms of three stress limit surfaces; the initial elastic yield surface, the failure surface and the residual friction surface. While the surfaces account for reduction in strength along different meridians as well as strain rate effects, the static compressive meridian surfaces are depicted in Figure 2. The failure surface, i.e., the ultimate strength of the concrete, is formed from material parameters including the compressive, tensile and shear strength of the concrete. The initial yield surface is then formed from user input fractions of the failure surface along the tensile and compressive meridian and additionally includes a cap that closes at the current pore crush pressure. A typical loading scenario can be described as follows, see also the arrows in Figure 2. The model is elastic until the stress reaches the initial yield surface, beyond which plastic strains evolve. The plastic strains together with the hardening properties of the concrete, given as input, are used to form an effective yield surface by interpolating between the initial yield surface and the failure surface. Similarily, when the stress reaches the failure surface a parametrized damage model governs the evolution of damage, driven by plastic strain, which in turn represents the post-failure stress limit surface by interpolating between the failure surface and the residual friction surface. For a fully damaged material, there is no meridian or strain rate dependence and shear strength is only supported under confined conditions, i.e., positive pressures.

4. Keyword format and standard parameter settings

The following is the keyword cards for the RHT concrete model in LS-DYNA, *MAT_RHT, and the parameters indicated as defaults correspond to a standard 35 MPa concrete presented in [7]. The units for this particular input is [mm, ms, kg, GPa], and further comments and explanations are given in subsequent sections.

Card 1	1	2	3	4	5	6	7	8
Varriable	MID	RO	SHEAR	ONEMPA	EPSF	B0	B1	T1
Type	A8	F	F	F	F	F	F	F
Default	NONE	2.314E-6	16.7	1.E-3	2.0	1.22	1.22	35.27

Card 2	1	2	3	4	5	6	7	8
Variable	A	N	FC	FS*	FT*	Q0	B	T2
Type	F	F	F	F	F	F	F	F
Default	1.6	.61	.035	0.18	0.1	0.6805	0.0105	0.0

Card 3	1	2	3	4	5	6	7	8
Varriable	E0C	E0T	EC	ET	BETAC	BETAT	PTF	
Type	F	F	F	F	F	F	F	
Default	3.E-8	3.E-9	3.E22	3.E22	0.032	0.036	0.001	

Card 4	1	2	3	4	5	6	7	8
Variable	GC*	GT*	XI	D1	D2	EPM	AF	NF
Type	F	F	F	F	F	F	F	F
Default	0.53	0.70	0.5	0.04	1.0	0.01	1.6	0.61

Card 5	1	2	3	4	5	6	7	8
Variable	GAMMA	A1	A2	A3	PEL	PCO	NP	ALPHA0
Type	F	F	F	F	F	F	F	F
Default	0.0	35.27	39.58	9.04	0.0233	6.0	3.0	1.1884

VARIABLE	DESCRIPTION
MID	Material identification. A unique number or label not exceeding 8 characters must be specified.
RO	Mass density.
SHEAR	Elastic shear modulus
ONEMPA	Unit conversion factor defining 1 Mpa in the pressure units used.
EPSF	Eroding plastic strain
B0	Parameter for polynomial EOS
B1	Parameter for polynomial EOS
T1	Parameter for polynomial EOS
A	Failure surface parameter A
N	Failure surface parameter N
FC	Compressive strength
FS*	Relative shear strength
FT*	Relative tensile strength
Q0	Lode angle dependence factor
B	Lode angle dependence factor
T2	Parameter for polynomial EOS
E0C	Reference compressive strain rate
E0T	Reference tensile strain rate
EC	Break compressive strain rate
ET	Break tensile strain rate
BETAC	Compressive strain rate dependence exponent (optional)
BETAT	Tensile strain rate dependence exponent (optional)
PFC	Volumetric plastic strain fraction in tension

VARIABLE	DESCRIPTION
GC*	Compressive yield surface parameter
GT*	Tensile yield surface parameter
XI	Shear modulus reduction factor
D1	Damage parameter
D2	Damage parameter
EPM	Minimum damaged residual strain
AF	Residual surface parameter
NF	Residual surface parameter
GAMMA	Gruneisen gamma
A1	Hugoniot polynomial coefficient
A2	Hugoniot polynomial coefficient
A3	Hugoniot polynomial coefficient
PEL	Crush pressure
PCO	Compaction pressure
NP	Porosity exponent
ALPHA	Initial porosity

5. Mathematical description

In the RHT model, the shear and pressure part is coupled in which the pressure is described by the Mie-Gruneisen form with a polynomial Hugoniot curve and a p-α compaction relation. For the compaction model, we define a history variable representing the porosity α that is initialized to $\alpha_0 > 1$. This variable represents the current fraction of density between the matrix material and the porous concrete and will decrease with increasing pressure. The evolution of this variable is given as

$$\alpha(t) = \max\left(1, \min\left(\alpha_0, \min_{s \le t}\left(1 + (\alpha_0 - 1)\left[\frac{p_{comp} - p(s)}{p_{comp} - p_{el}}\right]^N\right)\right)\right)$$

where $p(t)$ indicates the pressure at time *t*. This expression also involves the initial pore crush pressure p_{el}, compaction pressure p_{comp} and porosity exponent N. For later use, we define the cap pressure, or current pore crush pressure, as

$$p_c = p_{comp} - (p_{comp} - p_{el})\left[\frac{\alpha - 1}{\alpha_0 - 1}\right]^{1/N}$$

The remainder of the pressure (EOS) model is given in terms of the density and specific internal energy. Depending on user inputs, it is either governed by ($B_0 > 0$)

$$p(\rho, e) = \frac{1}{\alpha}\begin{cases} (B_0 + B_1\eta)\alpha\rho e + A_1\eta + A_2\eta^2 + A_3\eta^3 & \eta > 0 \\ B_0\alpha\rho e + T_1\eta + T_2\eta^2 & \eta < 0 \end{cases}$$

or ($B_0 = 0$)

$$p(\rho, e) = \Gamma\rho e + \frac{1}{\alpha}\, p_H(\eta)\left[1 - \frac{1}{2}\Gamma\eta\right]$$
$$p_H(\eta) = A_1\eta + A_2\eta^2 + A_3\eta^3$$

together with

$$\eta(\rho) = \frac{\alpha\rho}{\alpha_0\rho_0} - 1.$$

For the shear strength description we use

$$p^* = p / f_c$$

as the pressure normalized with the compressive strength parameter. We also use **s** to denote the deviatoric stress tensor and $\dot{\varepsilon}_p$ the plastic strain rate.

For a given stress state and rate of loading, the elastic-plastic yield surface for the RHT model is given by

$$\sigma_y(p^*, \mathbf{s}, \dot{\varepsilon}_p, \varepsilon_p^*) = f_c\sigma_y^*(p^*, F_r(\dot{\varepsilon}_p, p^*), \varepsilon_p^*)R_3(\theta, p^*)$$

and is the composition of two functions and the compressive strength parameter f_c. The first describes the pressure dependence for principal stress conditions $\sigma_1 < \sigma_2 = \sigma_3$ and is expressed in terms of a failure surface and normalized plastic strain as

$$\sigma_y^*(p^*, F_r, \varepsilon_p^*) = \sigma_f^*(\frac{p^*}{\gamma}, F_r)\gamma$$

with

$$\gamma = \varepsilon_p^* + (1-\varepsilon_p^*)F_e F_c .$$

The failure surface is given as

$$\sigma_f^*(p^*, F_r) = \begin{cases} A\left(p^* - F_r/3 + \left(A/F_r\right)^{-1/n}\right)^n & 3p^* \geq F_r \\ F_r f_s^*/Q_1 + 3p^*\left(1 - f_s^*/Q_1\right) & F_r > 3p^* \geq 0 \\ F_r f_s^*/Q_1 - 3p^*(1/Q_2 - \dfrac{f_s^*}{Q_1 f_t^*}) & 0 > 3p^* \geq 3p_t^* \\ 0 & 3p_t^* > 3p^* \end{cases}$$

in which $p_t^* = \dfrac{F_r Q_2 f_s^* f_t^*}{3\left(Q_1 f_t^* - Q_2 f_s^*\right)}$ is the failure cut-off pressure, F_r is a dynamic increment factor and

$$Q_1 = R_3(\pi/6, 0) \quad Q_2 = Q(p^*) .$$

In these expressions, f_t^* and f_s^* are the tensile and shear strength of the concrete relative to the compressive strength f_c and the *Q* values are introduced to account for the tensile and shear meridian dependence. Further details are given in the following.

To describe reduced strength on shear and tensile meridian the factor

$$R_3(\theta, p^*) = \frac{2(1-Q^2)\cos\theta + (2Q-1)\sqrt{4(1-Q^2)\cos^2\theta + 5Q^2 - 4Q}}{4(1-Q^2)\cos^2\theta + (1-2Q)^2}$$

is introduced, where θ is the Lode angle given by the deviatoric stress tensor **s** as

$$\cos 3\theta = \frac{27\det(\mathbf{s})}{2\bar{\sigma}(\mathbf{s})^3} \qquad \bar{\sigma}(\mathbf{s}) = \sqrt{\frac{3}{2}\mathbf{s}:\mathbf{s}} .$$

The maximum reduction in strength is given as a function of relative pressure

$$Q = Q(p^*) = Q_0 + Bp^* .$$

Finally, the strain rate dependence is given by

$$F_r(\dot{\varepsilon}_p, p^*) = \begin{cases} F_r^c & 3p^* \geq F_r^c \\ F_r^c - \dfrac{3p^* - F_r^c}{F_r^c + F_r^t f_t^*}\left(F_r^t - F_r^c\right) & F_r^c > 3p^* \geq -F_r^t f_t^* \\ F_r^t & -F_r^t f_t^* > 3p^* \end{cases}$$

in which

$$F_r^{c/t}(\dot{\varepsilon}_p) = \begin{cases} \left(\dfrac{\dot{\varepsilon}_p}{\dot{\varepsilon}_0^{c/t}}\right)^{\beta_{c/t}} & \dot{\varepsilon}_p \leq \dot{\varepsilon}_p^{c/t} \\ \gamma_{c/t}\sqrt[3]{\dot{\varepsilon}_p} & \dot{\varepsilon}_p > \dot{\varepsilon}_p^{c/t} \end{cases}.$$

The parameters involved in these expressions are given as (f_c is in *MPa* below)

$$\beta_c = \frac{4}{20+3f_c} \quad \beta_t = \frac{2}{20+f_c}$$

and $\gamma_{c/t}$ is determined from continuity requirements, but it is also possible to choose the rate parameters via inputs.

The elastic strength parameter used above is given by

$$F_e(p^*) = \begin{cases} g_c^* & 3p^* \geq F_r^c g_c^* \\ g_c^* - \dfrac{3p^* - F_r^c g_c^*}{F_r^c g_c^* + F_r^t g_t^* f_t^*}\left(g_t^* - g_c^*\right) & F_r^c g_c^* > 3p^* \geq -F_r^t g_t^* f_t^* \\ g_t^* & -F_r^t g_t^* f_t^* > 3p^* \end{cases}.$$

while the cap of the yield surface is represented by

$$F_c(p^*) = \begin{cases} 0 & p^* \geq p_c^* \\ \sqrt{1 - \left(\dfrac{p^* - p_u^*}{p_c^* - p_u^*}\right)^2} & p_c^* > p^* \geq p_u^* \\ 1 & p_u^* > p^* \end{cases}$$

where

$$p_c^* = \frac{p_c}{f_c} \qquad p_u^* = \frac{F_r^c g_c^*}{3} + \frac{G^* \varepsilon_p}{f_c}$$

The hardening behavior is described linearly with respect to the plastic strain, where

$$\varepsilon_p^* = \min(\frac{\varepsilon_p}{\varepsilon_p^h}, 1) \qquad \varepsilon_p^h = \frac{\sigma_y(p^*, \mathbf{s}, \dot{\varepsilon}_p, \varepsilon_p^*)\left(1 - F_e F_c\right)}{\gamma 3 G^*}$$

Here

$$G^* = \xi G$$

where G is the shear modulus of the virgin material and ξ is a reduction factor representing the hardening in the model.

When hardening states reach the ultimate strength of the concrete on the failure surface, damage is accumulated during further inelastic loading controlled by plastic strain. To this end, the plastic strain at failure is given as

$$\varepsilon_p^f = \begin{cases} D_1\left(p^* - (1-D)p_t^*\right)^{D_2} & p^* \geq (1-D)p_t^* + \left(\dfrac{\varepsilon_p^m}{D_1}\right)^{1/D_2} \\ \varepsilon_p^m & (1-D)p_t^* + \left(\dfrac{\varepsilon_p^m}{D_1}\right)^{1/D_2} > p^* \end{cases}$$

The damage parameter is accumulated with plastic strain according to

$$D = \int_{\varepsilon_p^h}^{\varepsilon_p} \frac{d\varepsilon_p}{\varepsilon_p^f}$$

and the resulting damage surface is given as

$$\sigma_d(p^*, \mathbf{s}, \dot{\varepsilon}_p) = \begin{cases} \sigma_y(p^*, \mathbf{s}, \dot{\varepsilon}_p, 1)(1-D) + D f_c \sigma_r^*(p^*) & p^* \geq 0 \\ \sigma_y(p^*, \mathbf{s}, \dot{\varepsilon}_p, 1)(1 - D - \dfrac{p^*}{p_t^*}) & (1-D)p_t^* \leq p^* < 0 \end{cases}$$

where

$$\sigma_r^*(p^*) = A_f\left(p^*\right)^{n_f}$$

Plastic flow occurs in the direction of deviatoric stress, i.e.,

$$\dot{\boldsymbol{\varepsilon}}_p \parallel \mathbf{s}$$

but for tension there is an option to set the parameter PFC to a number corresponding to the influence of plastic volumetric strain. If $\lambda \leq 1$ is used to denote this parameter, then for the special case of $\lambda = 1$

$$\dot{\boldsymbol{\varepsilon}}_p \parallel \mathbf{s} - p\mathbf{I}$$

This was introduced to reduce noise in tension that was observed on some test problems. A failure strain can be used to erode elements with severe deformation which by default is set to 200%.

6. Numerical example

An important application is the explosion protection of reinforced concrete and we here present numerical results from a close-in detonation of a reinforced concrete target initially performed in [8]. The parameters used for the RHT concrete are the same as given in the previous section and the model setup is shown in Figure 3. A 23.5 cm thick concrete plate with 0.1% reinforced content is subjected to a detonation of 1.25 kg Seismoplast at 10 cm distance. The rebar is modelled by steel beam elements along the mesh lines and ALE with Lagrangian-Eulerian coupling is used to simulate the blast and interaction with the concrete block.

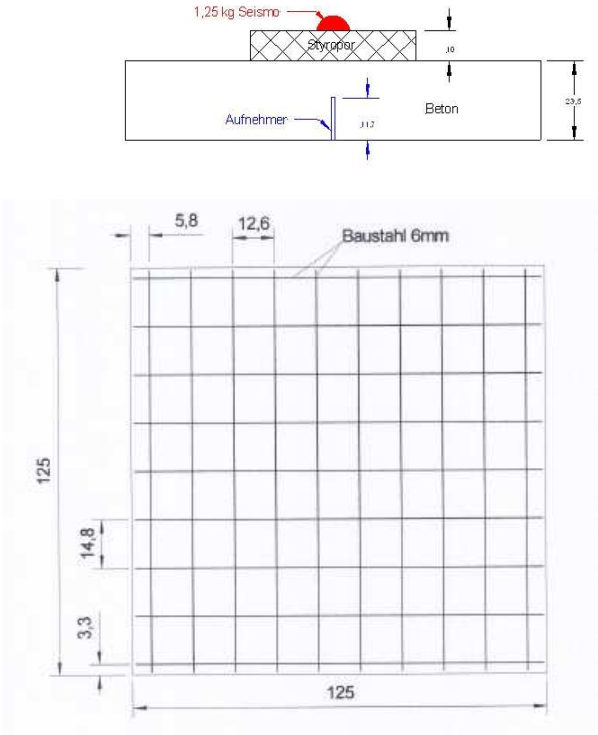

Figure 3 Model setup for contact detonation

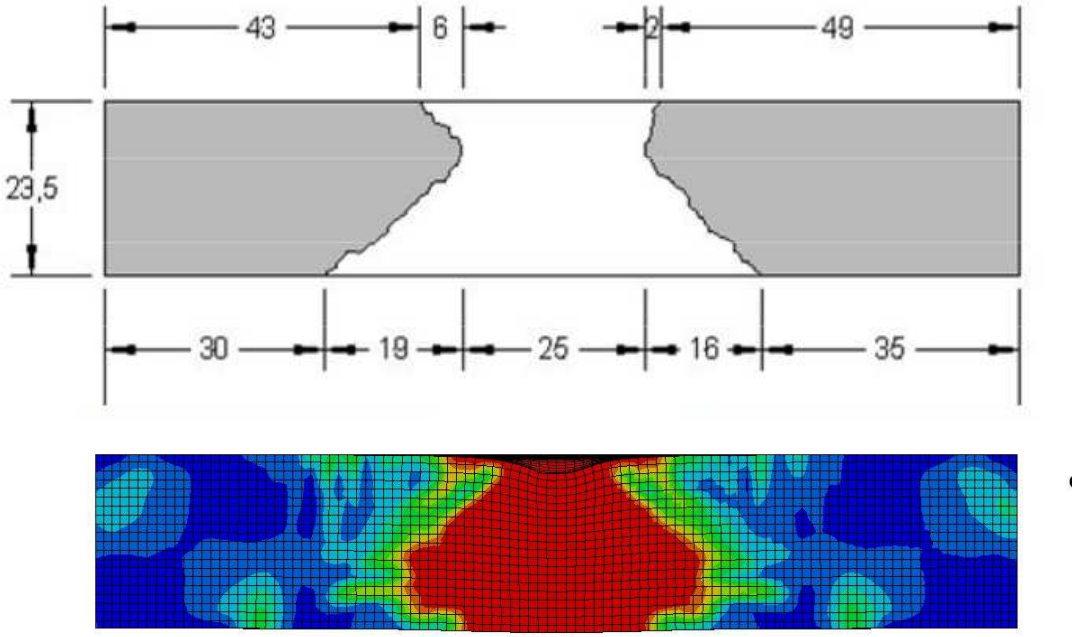

Figure 4 Experimental and simulation results of the contact detonation example

In Figure 4, the experimental and simulated results for this example is shown, where in the latter the damage parameter is fringe plotted. Red indicates fully developed damage (*D=1*) and except from not quite capturing the full extension of the breach the simulation is in qualitatively good agreement with the experiment. Furthermore, a pressure gauge was used to monitor the pressure in the center of the concrete block, the comparison of this measurement with the corresponding simulated result is shown in Figure 5. Again, the peak pressure is not quite reached but is still in the range of being acceptable.

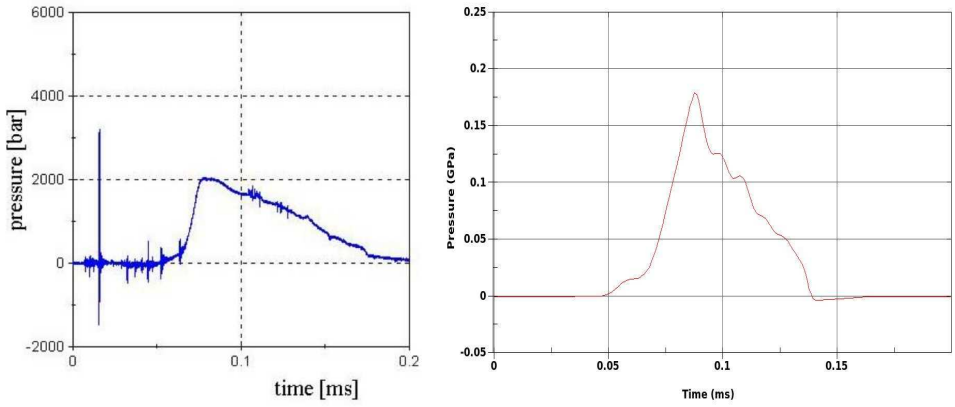

Figure 5 Monitored pressure in the center of concrete block, experiment and simulation.

7. Summary and outlook

The RHT model in LS-DYNA was presented together with sample data input and an application example. Because of the general interest of this model we believe that this will be a motivated contribution to the available set of concrete material models in LS-DYNA. The model features include

- Porous compaction treatment
- Ultimate strength specified independently in compression, tension and shear
- Elastic yield in percentage of ultimate strength
- Strain rate and meridian dependence
- Damage and failure

While the treatment in compression seems adequate, we have observed effects related to tensile softening that probably needs further work. It is well known, see [9,10] and references therein, that the tensile properties are important for the correct prediction of spalling, scabbing and crack prediction. A continuation in the development would be to extend the model to include an appropriate crack softening law as well as a more general strain rate treatment.

8. References

1. LS-DYNA Keyword User's Manual, Version 971, Volume I-II, Livermore Technology Software Corporation (LSTC), May 2007.
2. T. Holmqvist and G. Johnson, A computational constitutive model for concrete subjected to large strains, high strain rates, and high pressures, In: M. Murphy and J. Backofen (eds), 14th International Symposium on Ballistics, Quebec, 1993, pp. 591-600.
3. W. Riedel, K. Thoma, S. Hiermaier and E. Schmolinske, Penetration of reinforced concrete by BETA-B-500, numerical analysis using a new macroscopic concrete model for hydrocodes, In: SKA (ed), Proceedings of the 9th International Symposiumon Interaction of the Effects of Munitions with Structures, Berlin, 1999, pp. 315-322.
4. L. Malvar, J. Crawford, J. Wesevich and D. Simons, A plasticity concrete material model for DYNA3D, Int. J. Impact Eng., Vol. 19 (1997), pp. 847-893.
5. W. Hermann, Constitutive Equation for the Dynamic Compaction of Ductile Porous Materials, J. Appl. Physics, Vol. 40-6 (1969), pp. 2490-2499.
6. M. Caroll and A. Holt, Static and Dynamic Pore Collapse Relations for Ductile Porous Materials, J. Appl. Physics, Vol. 43-4 (1972), pp. 1626-1636.
7. W. Riedel, Beton unter dynamischen Lasten – meso- und makromechanische Modelle und ihre Parameter, EMI-Bericht 6/00, 2000.
8. W. Riedel, K. Thoma, C. Mayrhofer and A. Stolz, Engineering and numerical tools for explosion protection of reinforced concrete, Int. J. Prot. Struct. I, 2010, pp. 85-101.

9. J. Leppänen, Concrete subjected to projectile and fragment impacts: Modelling of crack softening and strain rate dependency in tension, Int. J. Impact Eng. 32 (2006) pp. 1828-1841.
10. H. Schuler, C. Mayrhofer and K. Thoma, Spall experiments for the measurement of the tensile strength and fracture energy of concrete at high strain rates, Int. J. Impact Eng. 32 (2006) pp. 1635-1650.